Moving towards green lubrication: tribological behavior and chemical characterization of spent coffee grounds oil

Jessica Pichler, Rosa Maria Eder, Lukas Widder, Markus Varga, Martina Marchetti-Deschmann & Marcella Frauscher

Published online: 29 May 2023.

Submit your article to this journal ☑

Article views: 328

View related articles ☑

View Crossmark data ☑

Taylor & Francis
Taylor & Francis Group

Moving towards green lubrication: tribological behavior and chemical characterization of spent coffee grounds oil

Jessica Pichler[a,b], Rosa Maria Eder [a], Lukas Widder [a], Markus Varga [a], Martina Marchetti-Deschmann [b] and Marcella Frauscher [a]

[a]AC2T research GmbH, Wiener Neustadt, Austria; [b]Institute of Chemical Technologies and Analytics, TU Wien, Vienna, Austria

ABSTRACT

With the EU aiming for net-zero greenhouse gas emissions by 2050, conventional production cycles must be transformed into cradle-to-cradle approaches. Spent coffee grounds are often dumped in landfills, with their potential as high-quality feedstock for biofuel or bio-lubricant production. Spent coffee grounds oil (SCGO) was investigated for its physicochemical properties while having more free acid groups compared to the reference polyalphaolefin 8 (PAO 8), which may cause faster oxidation. TGA results displayed comparable thermal stability of SCGO and PAO 8 for inert/oxidative atmosphere. The oil composition was characterized by ATR-FTIR, elemental analysis, and GC-EI-MS, where a higher oxygen content was found for SCGO, referring to functional ester/acid groups. The tribological behavior of SCGO was studied as lubricant base oil and as a 5% additive in PAO 8. The condition of fresh and tribologically used oils was investigated with High-Resolution-ESI-MS, and the worn surfaces were evaluated by light microscopy and topographic analysis. The results showed a superior friction coefficient of pure SCGO ($\mu = 0.092$) to PAO 8 ($\mu = 0.129$). The 5% SCGO additive in PAO 8 ($\mu = 0.095$) could significantly reduce friction compared to pure PAO 8 on an unpolished 100Cr6 surface.
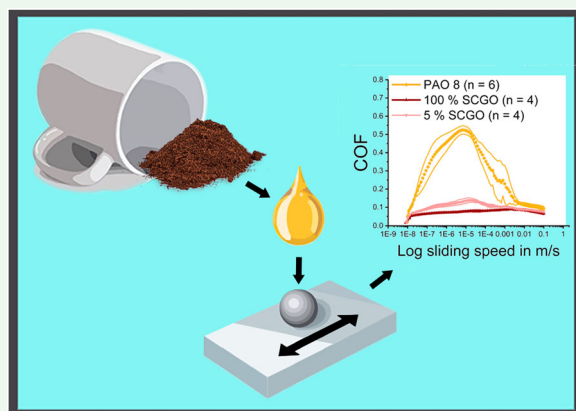
Introduction

Within the USA, the production of lubricants from renewable resources is facilitated by the USDA (U. S. Department of Agriculture) BioPreferred Program, where 139 bio-based product categories with mandatory purchasing requirements for agencies and contractors are currently listed, which is already 75 categories more than stated by Rudnick et al. in 2020 (1). These categories include engine oils, chain- and cable lubricants, transformer fluids, metalworking fluids, gear lubricants, intermediates, and additives for lubricant formulation and come with a minimum renewable biological content, which for lubricants lies within 25% for (wheel bearing and chassis) greases and 95% for transformer fluids (vegetable-oil based) (2). However, similar pull marketing strategies are currently missing in the EU.

In Europe, the year 2021 marked the beginning of a more sustainable future by bringing the European Green Deal (Regulation (EU) No 2018/1999 of the European Parliament and of the Council) (3) to life. Along with the Circular Economy Action Plan, the 2030 Climate Target Plan, and the Fit For 55 package, addressing the 55% of net greenhouse gas emission

reduction by 2030 compared to 1990 levels, Europe is heading towards climate neutrality by 2050 (*4*).

In other words, standard lubrication systems mainly of petroleum-based origin need to be adapted to reach the goals addressed by the Green Deal, such as achieving an energy portion of 32.5% from renewable sources by 2030 (*3*). There is an increasing interest in the generation of lubricants from alternative sources, e.g. lubricants from used cooking oils (UCO). However, nearly 90% of these UCOs are used as UCO methyl esters (UCOME) for biodiesel (*5*).

Within the European Union, Directive (EU) 2018/851, an amendment to Directive 2008/98/EC on waste, provides improved waste management requirements and guidance addressing the whole life-cycle of products, thus, promoting the idea of a truly circular economy (*6*). Considering waste as a valuable resource can reduce its environmental impact, which is necessary to protect, preserve and improve the quality of the environment. The sustainability roadmap of the European Circular Economy package aims at a recycling rate of 55% of municipal waste by 2025, a separate collection of hazardous household waste by 2022, and bio-waste by 2023 (*7*). The Directive advises member states to take responsibility for preventing waste generation in the first place or otherwise to implement suitable long-term recovery strategies for re-using and recycling waste material. These include processes that promote and support sustainable production and consumption, design-to-recycle or reuse, food waste reduction in primary production and food donation, reduction of industrial waste products, and the determination of primary sources of natural and marine litter (*6*).

In this regard, within the scope of this work, the focus was on SCGO as a sustainable, waste- and bio-based lubricant, or lubricant additive, which could contribute to achieving the climate goals set in the European Green Deal. Furthermore, it should comply with the concept of a circular economy and meet the high standards of the EU Ecolabel (*8*).

According to a study, almost 10,200,000 tonnes of coffee is consumed globally per year (2020); for Austria, this number is 46,000 tonnes (2018), which results in 10.1 kg (2019) of coffee per person annually (*9*). Making a rough estimation for the Austrian market, with a recycling rate of just 10%, 4,600 tonnes of spent coffee grounds (SCGs) could be collected annually, yielding 690 tonnes of SCGO (based on 15% oil content of dry SCGs).

SCGs, with a lipid content of 11-20% (dry weight basis) (*10*), are often considered a sustainable feedstock for biodiesel production (*10–14*). Efthymiopoulos (*10*) is providing a comprehensive study investigating the reuse of SCGs as an energy source, considering that SCGs contain compounds, which may be seen as pollutants when disposed of at landfills (*10*). By-products from coffee processing, such as SCGs and raw coffee husks, are described as phytotoxic due to components such as caffeine, tannins, and other polyphenols (*15,16*). An evaluation of the toxicity and/or biodegradability of SCGO could not yet be found in the literature.

Comparing the efficiency of different extraction methods, such as Soxhlet extraction (SE), ultrasonic extraction and microwave-assisted extraction (MAE), on dried SCGs with n-hexane and petroleum benzene SE provides the highest total yield of SCGO but cannot keep up with the low amounts of solvents and extraction time needed for the other methods. With supercritical fluid extraction (SFE) with CO_2, a change in fatty acid composition depending on temperature, pressure, type of modifier and modifier volume could be observed (*20*). These insights were confirmed when SCGs were extracted with MAE and conventional SE, where MAE seemed far superior with a 24-fold increase in efficiency, implying that less solvent per gram oil collected is needed (*21*). Another approach comprises enzymatic hydrolysis of crude SCGO to free fatty acids (FFAs) and further esterified with trimethylol-propane (TMP), which resulted in TMP esters useful for bio lubricant production (*22*).

Al-Hamamre et al. (*18*) extracted dried SCGO with different polar (isopropanol, ethanol, and acetone) and non-polar (toluene, chloroform, hexane, and n-pentane) solvents by SE before further converting free fatty acids to fatty acid methyl esters by two-step transesterification. Hexane showed the highest oil yield after 30 min of extraction with 15.28%, a low free fatty acid content and acid value. Based on these results, the herein-used extraction parameters were chosen since the proposed process is well-established.

Although many studies address different extraction methods and oil yield from SCGs, as highlighted above, only one is investigating SCGO tribologically: Grace et al. (*17*) tested SCGO as base oil with 1, 2.5 and 5 wt% of phosphonium-based ionic liquids (ILs) as an additive in a steel-steel contact on a reciprocating block-on-flat tribometer. The SCGO ILs are compared to a fully formulated commercially available wind turbine gearbox lubricant. In these experiments, ILs as additives to SCGO could reduce wear values and wear volume, and some could also reduce the coefficient of friction (COF).

Since a high potential of SCGO as a base lubricant or additive component can be assumed, tribological behavior is the main focus of this work. At first, the power of SCGOs to contribute to the greening of

industrial applications was assessed by a comprehensive SCGO life-cycle assessment from production to application. A further step was optimizing the extraction method to ensure the reproducibility and stability of the molecular content and its distribution throughout multiple extraction batches. The obtained SCGO was thoroughly examined regarding its physicochemical properties and characteristic qualities.

In this work, we want to increase knowledge in the tribological field and further evaluate the properties of SCGO in terms of friction and wear. Therefore, we applied tribological testing in steel/steel contact primarily to determine the possible operational range and operating conditions of SCGO in industrial applications and compared our findings to well-established PAO base oil. Additionally, a life cycle assessment comprised an upscaling from lab scale to industrial production to highlight critical aspects of environmental and toxicity impacts and energy consumption.

Experimental

Materials and consumables

SCGs from different companies (Amaroy Wiener Mischung/ Hofer, Eduscho Gala Nr. 1/Eduscho, and Spezial/ J. Hornig) were collected. PAOs were supplied by OMV, Austria. N-hexane (≥ 99%; Roth, Germany) was used for extraction, sulfanilic acid (≥ 99%; VWR Chemicals, Germany) and benzoic acid (≥ 99.5%, Merck, Germany) purchased through Elementar Analysensysteme GmbH were used as standards for CHNSO elemental analysis. Dichloromethane (DCM; ≥ 99.9%; Sigma-Aldrich, USA) and N,O-Bis-(trimethylsilyl)trifluoroacetamide with trimethylchlorosilane (BSTFA + TMCS; 99%; Sigma-Aldrich, Switzerland) were used for GC-MS analysis; the latter acted as a derivatization agent. For Karl-Fischer titration solution HYDRANAL™ – Coulomat AG-Oven (Honeywell Fluka, Germany) was used. EMSURE® KOH pellets for acid number (AN) evaluation were obtained from Supelco, Germany (≥ 85.0%). For High-Resolution (HR)-MS analyzes, isopropanol (≥ 99.95%; Roth, Germany) and methanol (≥ 99.9%; Supelco, Germany) were used. Material surfaces were cleaned threefold with isopropanol (≥ 98%; VWR, Austria), acetone (≥ 99%; VWR, Austria), and petrol ether (≥ 99.5%; VWR, France).

Sample collection

Collected SCGs were dried in an oven for 24 h at 105 °C to remove moisture. Soxhlet extraction (SE), with n-hexane as the organic solvent, was chosen to extract crude oil from the SCGs. About 20 g of dried SCGs were weighed into a thimble in the Soxhlet extraction chamber. Extraction was performed at 140 °C device temperature (after a few rounds of optimization due to heat loss within the setup hot plate + silicon oil bath) with 200 ml of n-hexane under reflux until the solvent in the extraction chamber was fully clear/colourless (5-8 h). Afterwards, the solvent was removed on a rotary evaporator (Basis HEI-VAP ML, Heidolph, Germany) at 334 mbar, 100 rpm and 50 °C for 90 min.

The moisture content of SCG was calculated from wet weight (g) and dry weight (g) as the amount of water (g) divided by the total weight (g). The crude oil yield was calculated as the amount of oil extracted (g) divided by the amount of dry SCGs used (g).

Characterization methods

Physicochemical properties of SCGO

Rheology measurements were carried out on a rheometer (MCR 302, Anton Paar, Austria) with 50 mm cone-plate measuring geometry within shear rates from 0.1 to 100 s^{-1} and a temperature of 30 °C to determine similar viscosity ranges for SCGO and PAO reference oils and choose the best rheological reference fit for SCGO. The matrix of all executed measurements is shown in Table 1.

The water content was determined according to DIN 51777 (direct and indirect method) by Karl-Fischer (KF) titration (831 KF Coulomat and 890 Titrando, Metrohm Inula GmbH, Austria), the AN (mg KOH/g) was evaluated according to DIN 51558-2. The thermal stability was examined up to 450 °C under a synthetic air atmosphere and up to 500 °C under an N_2 atmosphere by thermogravimetric analysis (TGA) and differential scanning calorimetry (DSC)/differential thermal analysis (DTA) on a thermo-gravimetric analyser (STA 449 F3 Jupiter, Netzsch, Germany) with a heating rate of 10 °C/min and initial sample weights ~10 mg in Al crucibles. The derivative (DTG) of the TG-signal over time was drawn, and a Savitzky–Golay filter was applied.

Table 1. Experimental matrix for SCGO and PAO 8, selected as reference lubricant.

wt%		SCGO 100			SCGO 5			Reference PAO 8 100		
No.		1	2	3	1	2	3	1	2	3
Rheometer	Stribeck	X	X	x	x	x	x	x	x	x
	oscillating	X	X	-	x	x	-	x	x	x
Nanotribo-meter	oscillating	X	X	x	x	x	x	x	x	x
Physico-chemical	IR	X	–	–	–	–	–	x	–	–
	Viscosity	X	–	–	x	–	–	x	–	–
	AN	x	–	–	–	–	–	x	–	–
	Water	x	–	–	–	–	–	x	–	–
TGA/DSC		x	–	–	–	–	–	x	–	–
CHNSO	CHNS	x	X	x	–	–	–	x	x	x
	O	x	X	x	–	–	–	x	x	x

Determination of oil composition

The elemental composition of the oil was characterized by CHNSO elemental analysis (varioMACROcube, elementar, Germany) with He as carrier gas at 1150 °C (CHNS-mode) or 1170 °C (O-mode). Sulfanilic acid was used as the standard substance for CHNS mode, and benzoic acid was used as a standard substance for O mode. Liquid samples were weighed in tin capsules, tightly sealed under Argon atmosphere, and measured in doublet. ATR-FTIR was recorded in a spectral range of 4000-600 cm^{-1} and a wavenumber resolution of 4 cm^{-1} (Tenor 27, Bruker Optik GmbH, Germany).

GC-EI-MS (TQ8040; Shimadzu, Germany) determined the fatty acid distribution with AOC-20i + s autosampler diluted four wt% in dichloromethane with 18 wt% of BSTFA as a silylation agent. The sample was silylated for one h at 70 °C.

Table 2 shows the measurement conditions of the GC-MS analysis. All samples were analyzed twice in independent repetitions.

Tribological experiments

SCGO was tested as a base oil (100%) and five wt% diluted in PAO 8 (SCGO as additive). Tribological tests were conducted on a rheometer (MCR302) and nanotribometer (NTR[3]) from Anton Paar, Austria. The rheometer tribo-measurements were executed in unidirectional rotation and rotational oscillating motion with a 12.7 mm diameter 100Cr6 ball vs 100Cr6 base bodies in a ball-on-three-discs (45°) geometry. The rotational motion was used to determine the frictional behavior of the lubricated interface as a so-called Stribeck curve. The rotational oscillating motion was used to compare friction and wear to results obtained using the nanotribometer with a linear oscillating motion. The parameters of the tribological tests are given in Table 3.

The nanotribometer measurements were performed linearly oscillated using a 2 mm diameter 100Cr6 ball on various base bodies (ball-on-disc setup). The base

bodies included: (a) unpolished 1.4301 stainless steel plates (from now on referred to as S-SSUP); (b) unpolished 100Cr6 discs (S-CRUP); and (c) polished 100Cr6 plates (polished in-house; S-CRP) and are summarized in Table 4. Used base bodies exhibit varying surface roughness to determine more detailed insight into SCGO tribological behavior.

Since the rheometer and nanotribometer have different system setups, the rheometer parameters were adjusted to apply an identical Hertzian contact pressure in both experimental designs. The stroke distance on the rheometer for rotational oscillation was calculated through the angular deflection of 111.24 mrad (equals a stroke of 500 µm), dependent on the instrument geometry.

Tribological tests on the nanotribometer and rheometer were carried out for 900 cycles per minute for 15 and 120 min. Fifty data points were collected tip-to-tip (25 data points per stroke) per cycle on the nanotribometer and 20 data points (10 per stroke) on the rheometer. The data was then treated and reduced as follows: the absolute friction values of a cycle were taken and reduced to 60% of the mean range of each stroke to discard acceleration and deceleration motion data from the stroke-end turning positions. The data was further reduced to one value per cycle. Hence, 900 (nanotribometer) and 7200 (rheometer) values in total averaged over (a) three (nanotribometer) and (b) two (rheometer) measurement repetitions. Finally, the mean value with a standard deviation of (a) three and (b) two measurements, plus the 1st decile ($Q_{0.1}$) and

Table 2. GC-MS instrument and method parameters for SCGO characterisation.

Properties	Specification
Carrier gas	Helium
Linear velocity	51.6 cm/s
Column dimensions	5% diphenyl/95% dimethyl polysiloxane, 30 m × 0.25 mm × 0.25 µm
Injector	Type: PTV Split (25:1) Injection Volume: 1 µl
Oven temperature ramp	1 min hold at 60, 10 °C/min to 300 °C, hold for 20 min
Transfer temperature	250 °C
MS source temperature	200 °C

Table 3. Parameters for the rotational and linear tribological experiments on the rheometer and nanotribometer.

	Rheometer		Nanotribometer
Operational Mode	Unidirectional rotation	Rotational oscillation	Linear oscillation
Load F_N in N	5	20.17	1
Temp. in °C	30	30	25
Hertzian Contact Pressure in GPa	–	1.37	1.37
Distance in µm	–	500	500
Frequency in Hz	–	1	1
Sliding speed in m/s	10^{-8}–0.1	10^{-3}	10^{-3}

Table 4. Material surfaces and properties for tribological measurements.

Material	Abbrev.	Surface roughness R_q in µm	Reduced valley depth S_{vk} in µm	Valley material portion S_{Mr2} in %
1.4301 stainless steel	S-SSUP	0.156 ± 0.035	0.61 ± 0.14	83.24 ± 1.12
100Cr6	S-CRUP	0.086 ± 0.007	0.16 ± 0.01	82.51 ± 0.53
100Cr6	S-CRP	0.007 ± 0.002	0.01 ± 0.00	90.19 ± 1.30

90% quantile ($Q_{0.9}$) are displayed in Figure 6. The standard deviation of uncertainty within measurement repetitions is given as error bars in the figures. For the oscillatory rheometer measurement, the wear scars of the three tested oils were further evaluated with two-dimensional microscopy and three-dimensional topographic analysis with values displayed as a mean of six surface characterizations (three discs times two runs).

For the rheometer oscillatory measurements composition of the three oils and possible ageing effects during the tribological experiments were investigated by High-Resolution (Orbitrap)-Electrospray Ionization (ESI)-MS in positive and negative ion mode. The pre- and post-rheometer test oil samples were diluted 1:1000 in methanol/isopropanol (1:1 wt%) for further mass spectrometric examinations.

Relevant surface roughness parameters for the oil retention volume, the reduced valley depth S_{vk} and the valley material portion S_{Mr2} were determined by three individual topography measurements of 600 μm x 600 μm scan size (Leica DCM8, Leica Microsystems GmbH, Switzerland) via the area material ratio curve or Abbott-Firestone curve and are given in Table 4.

Results and discussion

SCGO extraction

The crude oil yield varied between 9.5 wt% to 20.3 wt% of dry SCGO with a mean yield of approximately 14 wt%. The moisture content of the wet SCGs (before drying in the oven) showed a mean of 70 wt% (ranging from 60 wt% to 75 wt%) for different SCG types. A mixture of three different extraction batches and five SCG types was used for further analysis.
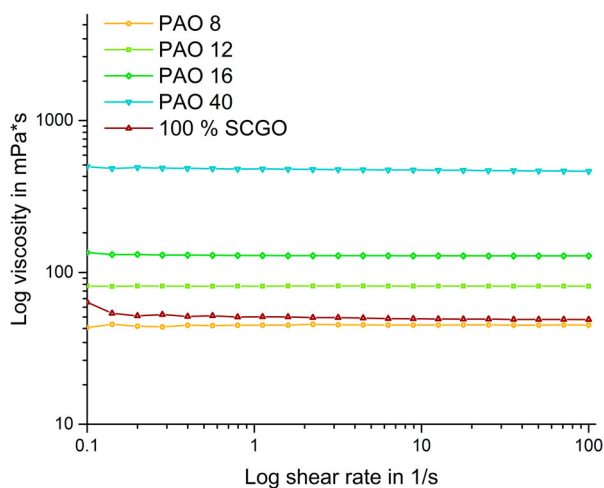

Figure 1. Dynamic viscosity measurement of different viscous PAOs and 100% SCGO over a shear rate of 0.1–100 s^{-1}.

Table 5. Chemical properties of SCGO and elemental composition.

Oil Type	AN in mg KOH/ g	Water in wt %	Elemental analysis in wt%				
			C	H	N	S	O
PAO 8	0.05	0.007	85.2	14.1	0.4	0.1	0.0
SCGO	4.83	0.029	75.4	11.5	1.1	0.2	9.9
SCGO (18)	7.38	–	79.1	11.1	0.2	0	9.6[a]

[a]Calculated.

Physicochemical properties of SCGO

First, the SCGO's viscosity was characterized to identify a matching reference oil. The dynamic viscosity of different viscous PAOs (Figure 1) was measured on the rheometer, with PAO 8 being the best fit. Over the range of 0.1–100 s^{-1} at 30 °C the mean viscosity of PAO 8 was at 44.92 mPa·s and for 100% SCGO at 51.08 mPa·s, which coincides with viscosity values for SCGOs already described in the literature: The kinematic viscosity of SCGO at 40 °C was determined between 49.6-55.5 mm²/s and 9.4-9.9 mm²/s at 100 °C when extracted with n-hexane as the solvent (13,17,18). The dynamic viscosity resulted in 60 mPa·s at 40 °C and 8.7 mPa·s at 100 °C (18).

In Table 5, the chemical properties of the SCGO and PAO 8, such as the AN, the water content, and the elemental content of carbon, hydrogen, nitrogen, sulfur, and oxygen, are given. A low AN, which determines the number of carboxylic acid groups within the oil, accounts for a more oxidatively stable oil since it contains fewer free fatty acids. The AN of SCGO measured within the scope of this work is relatively low, with a value of 4.83 mg KOH/g and considerably lower than the value of 7.38 mg KOH/g reported by Al-Hamamre et al. (18) which could be due to different oil extraction procedures. Nitrogen, sulfur, and hydrogen contents differ slightly for PAO 8 and SCGO; a more significant difference is visible for the oxygen content of 9.92% for SCGO (deriving from ester groups) and 0.02% for PAO 8 (a pure hydrocarbon liquid). The water content for both oils is below 0.05 wt%.

Previous research studies have found the following properties of SCGO: cloud point of 12.2 °C (ASTM D5773), pour point of 7.0 °C (ASTM D5949), lubricity at 60 °C of 180 μm (ASTM D6079), specific gravity of 0.94 (AOCS Cc 10c-95), and rancimat index (110 °C; indicating oxidative stability; EN 15751) of 8.4 h (13). The density at 23 °C is 0.85 g/cm³, and the thermal degradation of SCGO up to 300 °C is below one wt% (17). With the use of different extraction solvents, the saponification value of SCGO varies from 171 to 223 mgKOH/g, the acid number from 6.5–12.8 mgKOH/g, the ester number between 167–214 mgKOH/g, the free fatty

acid content from 3.3–6.4%, and the dielectric constant was within the range of 2.6-25.7. The refractive index is at approximately 1.47 (18,19).

PAO 8 and SCGO were analysed using simultaneous thermal analysis (TGA and DSC), showing the mass loss and the change in the heat flow of a sample as a function of time in an inert atmosphere (N_2) up to 500 °C and synthetic air up to 450 °C with an onset temperature of mass loss defined as 0.2% within one centigrade. The oxidation sensitivity of the specimen holder is influenced by temperature limitations for the synthetic air atmosphere, which is not the case with N_2-atmosphere. Therefore, mass loss is not available for the whole temperature range of synthetic air. For both atmospheres, at least one intermediate is formed with SCGO, which was not further chemically analysed but might include the degradation of different saturated and unsaturated fatty acids at different temperatures before complete degradation.

When the samples were pyrolyzed in N_2-atmosphere (Figure 2), the onset temperatures for thermal decomposition of PAO 8 with 278.05 °C and SCGO with 274.04 °C are well comparable, the endothermic change in the DSC signal also indicates this process.

When synthetic air was applied (Figure 3), oxidative degradation of PAO 8 occurred at 244.68 °C, which is lower than the onset value of 281.28 °C for SCGO (the value might be shifted due to intermediate formation).

Here, the SCGO forms multiple intermediates visible by the 1st derivative of the TGA signal (DTG) before complete combustion, again possibly deriving from the stepwise decomposition of different saturated and unsaturated fatty acids. The DSC curve indicates an exothermic reaction (upward peak).

Vegetable oils as lubricant base oils are known to have significant weaknesses in their oxidation stability, hydrolytic stability, and low-temperature properties. Saturated fatty acids are more thermodynamically stable than unsaturated fatty acids, which leads to a higher melting temperature and better oxidation stability. The bent structures of the unsaturated fatty acid moieties (such as oleic, linoleic or linolenic acid) of the SCGO are responsible for the liquidity at ambient temperature. The higher the amount of unsaturated fatty acids within the oil, the better the low-temperature properties, but the poorer the oxidative stability (1).

In Rudnick et al. (1), it is stated that the evaporation rates (in the absence of oxygen) of TGA of vegetable oils are significantly lower than those of iso-viscous hydrocarbon and synthetic base fluids. Furthermore, for the volatility in the presence of oxygen, rates were lower for vegetable oils compared to mineral oils. This observation could be confirmed with SCGO, neither for evaporation nor oxidative decomposition, since the
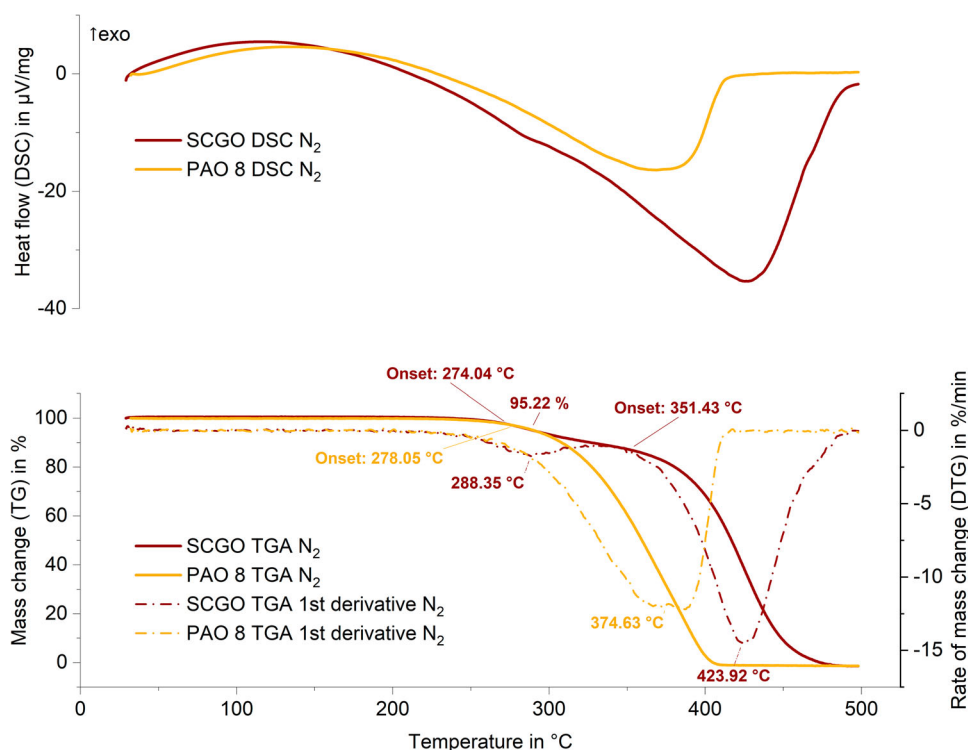

Figure 2. TGA (bottom, full line) and 1st derivative (dotted line) and DSC (top) **thermograms** in N_2 of SCGO and PAO 8. The heating rate is 10 °C/min.
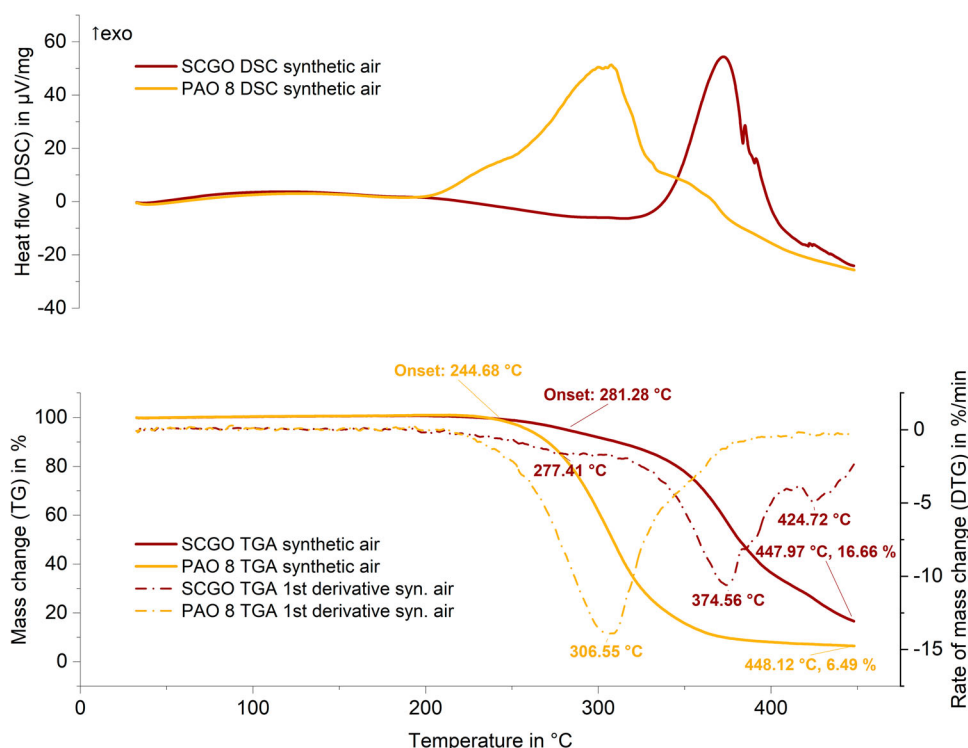
Figure 3. TGA (bottom, full line) and 1st derivative (dotted line) and DSC (top) **thermograms** in synthetic air of SCGO and PAO 8. The heating rate is 10 °C/min.

thermodynamic stability of PAO 8 and SCGO were always comparable. Moreover, they described a degradation mechanism of most oils with at least two steps, also present in SCGO. The good overall temperature stability of the SCGO might be due to a more balanced ratio of saturated to unsaturated fatty acids compared to other vegetable oils.

Figure 4. ATR-FTIR results: SCGOs compared to PAO 8 and PAO 40. M1: 100% SCGO as a mixture of two different coffee ground types; M2: 100% SCGO as a mixture of four different coffee ground types; P1: single-batch extraction: 100% SCGO of the same coffee ground type.

For ATR-FTIR (Figure 4) and GC-MS (Table 6), pure (P1: one extraction, one SCG type) and mixtures (M1: three extractions, two SCG types; M2: three extractions, five SCG types) of different SCGOs from the three coffee grounds sources were studied to identify their chemical structure. Only minor variations were observed when comparing pure SCGO to mixtures of SCGO. Therefore, a combination of different SCGO extractions was used for further investigations to increase the sample volume. Moreover, SCG as a valuable waste resource will also most likely not be available as a homogeneous single-kind fraction when disposed of at coffee shops and the like but rather as a mixture of various SCG types and grades.
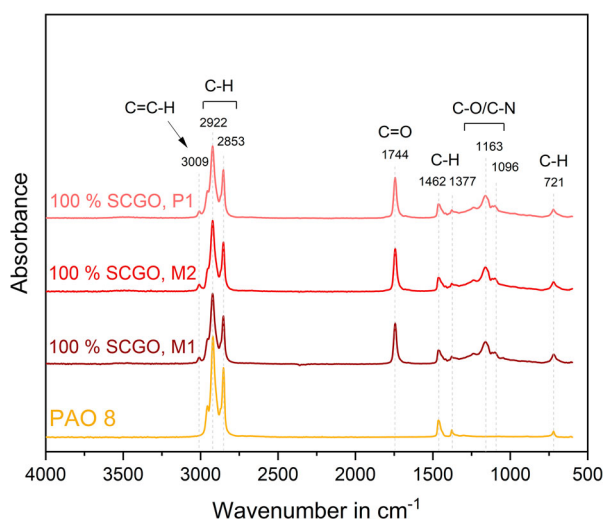
The wavelength range of 1300-1000 cm^{-1}, as seen in Figure 4, is typical for C–O stretching vibrations characteristic for ester bonds related to the C = O carbonylic stretching vibrations at 1744cm^{-1} of ester groups. The vibration band at 1163 cm^{-1} reveals the presence of C–N amine bond stretching. Absorption at these wavenumbers is only found in SCGOs due to a lack of ester and amine structures in PAOs. The presence of C–H groups is shown by vibrations at 721 cm^{-1} (rocking; seen only in long chain alkanes), 1462 cm^{-1} (scissoring), 1377 cm^{-1} (methyl rocking), as well as 2922 and 2853 cm^{-1} (stretching), all appearing in the three SCGOs and synthetic PAO-based oil. The signal at 3009 cm^{-1}, which is only found in SCGO, represents

Table 6. Fatty acid distribution of SCGO detected by GC-MS and compared to literature.

| Fatty acid | FA code | Peak area % | | | | |
| | | Present work | | | Literature | |
		100% SCGO, M1	100% SCGO, M2	100% SCGO, P1	(22)[a]	(21)
Palmitic	C16:0	44	41	43	43	41.9
Stearic	C18:0	11	10	8	14	5.65
Oleic	C18:1	10	11	9	10	5.29
Linoleic	C18:2	11	17	16	31	20.92
Arachidic	C20:0	5	4	3	–	–
Arachidonic	C20:4	4	4	3	–	–
Docosanoic	C22:0	1	1	–	–	–
Others	–	–	–	–	2	–
Sat./unsat.	–	2.41	1.72	1.95	1.39	1.81

[a]Source is transesterified.

C = C–H stretching. With ATR-FTIR, a distinction between the three types of SCGO is impossible.

GC-MS values for fatty acid compositions vary slightly in literature and the herein performed measurements, as seen in Table 6, possibly depending on varying sample preparation procedures and measurement parameters.

The analysed fatty acid composition of SCGO shows a key peak for palmitic acid (n-hexadecanoic acid) with an area of 41-43%. According to the literature, the composition will vary slightly with the type of coffee grounds used (Arabica or Robusta) (22); here, mixtures of Arabica and Robusta are used. Ahangari et al. (20) showed that different operational conditions (e.g. extraction conditions) have quite a substantial impact on the fatty acid distribution as well.

Tribological behavior

Stribeck curves

Unidirectional rotation experiments were carried out on the rheometer on the S-CRUP surface, showing the variation of the COF over a sliding speed range from $8*10^{-9}$ m/s to 10^{-1} m/s, providing the Stribeck curve. The COF is given as an average of two measurements. The first bend of the curves of PAO 8, 100% SCGO, and 5% SCGO (Figure 5) indicates a transition from static friction to sliding friction (around 10^{-8} m/s). The second regime, where the COF increases, identifies as the boundary lubrication regime before the curves bend again and mixed lubrication starts. Boundary lubrication occurs until the maximum COF of the curves, which is between approx. $1.2*10^{-8}$–$6.3*10^{-6}$ m/s for PAO 8, $1.5*10^{-8}$ m/s to $5*10^{-3}$ m/s for 100% SCGO, and $1.4*10^{-8}$ m/s to $1.7*10^{-5}$ m/s for 5% SCGO. After the largest COF, the mixed lubrication regime is entered. An additional increase of COF with increasing sliding speeds due to hydrodynamic lubrication was not observed.
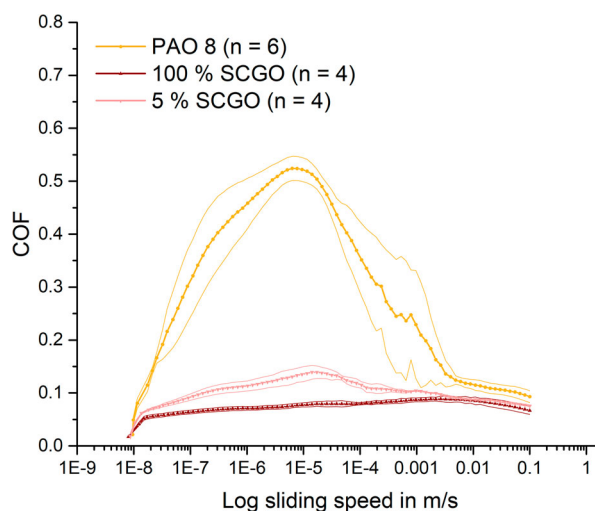
Figure 5. Stribeck curve of rheometer experiments using PAO 8, 100% SCGO and 5% SCGO in PAO 8 on S-CRUP.

The dedicated maximum COF (μ_{max}) of 100% SCGO at 0.089 is significantly lower than that of PAO 8, being 0.524, which can be attributed to the friction-reducing properties of ester groups within this type of oil. Especially noteworthy is the low COF of 5% SCGO in PAO 8 of 0.139, indicating that SCGO works well as a boundary friction modifier additive.

Furthermore, the existence of wear also indicates boundary lubrication, which was visible for all three oil types. However, surface roughness is crucial in wear estimation due to the short measurement duration and low friction force applied. Wear volume and wear depth could not be adequately estimated for the S-CRUP surface. Thus, only surface polishing effects could be observed; the wear estimations are subjected to considerable fluctuations by the mean shift of unworn surface reference caused by the surface roughness. The mean wear scar depth of the different measurements lies within 0.02-0.13 μm Rq, which is relatively low and within the range of the original surface roughness.

Oscillating movement

The oscillating tribological experiments were carried out on dissimilar materials with varying surface roughness. Friction and wear scars are compared on samples from rheometer (ball on three discs) and nanotribometer (ball on disc) experiments. The COF was recorded for all measurements. Additionally, wear depth and volume were determined using topography measurements.

A comparably lower COF for 100% and 5% SCGO than for PAO 8 is visible and will be discussed in detail in the following sub-chapter. An overview of the COF on the different surfaces of all executed nanotribometer and
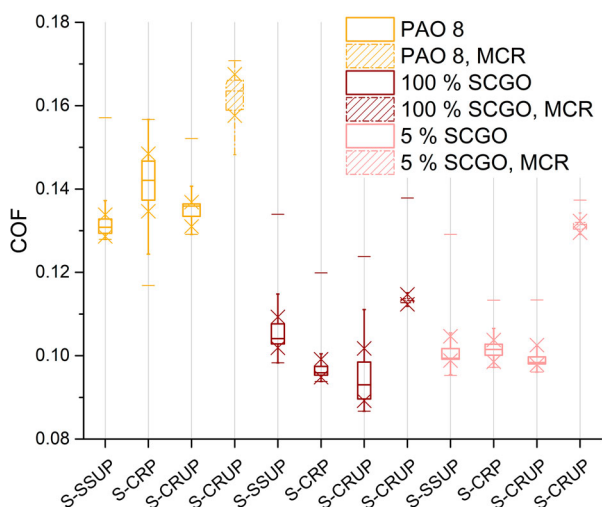
Figure 6. Box-and-whisker-plot of COF on different surfaces of nanotribometer and rheometer measurements. The box is giving the lower (25%) and upper (75%) quartile, whiskers are used to represent all samples lying within 1.5 times the interquartile range (IQR). Median line (thick horizontal line), quantiles $Q_{0.1}$ and $Q_{0.9}$ (cross), and maximum and minimum values (thin horizontal line) are displayed.

rheometer measurements is given in a box-and-whisker plot in Figure 6.

Nanotribometer experiments on S-SSUP samples. For the unpolished S-SSUP steel plates used in nanotribometer experiments (Figure 7), the friction coefficients of 5% SCGO in PAO 8 and 100% SCGO are in close proximity. The friction values for PAO 8 are the highest ($\mu_{mean} = 0.126$) compared to 100% SCGO ($\mu_{mean} = 0.102$) and 5% SCGO ($\mu_{mean} = 0.097$). After 15 min of measurement duration, there still is a decrease of COF observable for all three lubricants, which can be related to the system still being in the run-in phase.
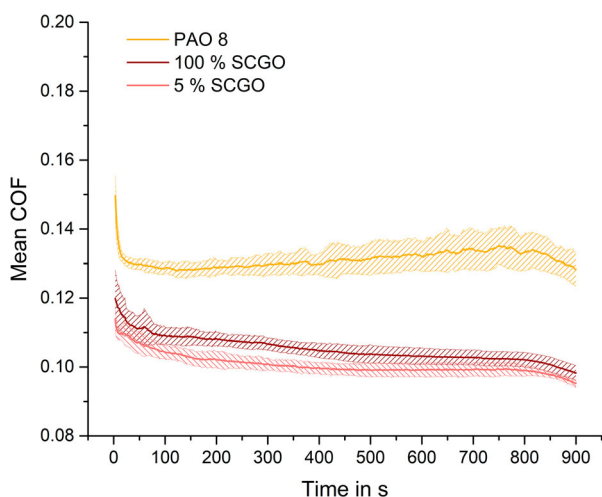

Figure 7. Friction values of nanotribometer experiments of different oils on unpolished S-SSUP given with standard deviation between data sets ($n = 3$).
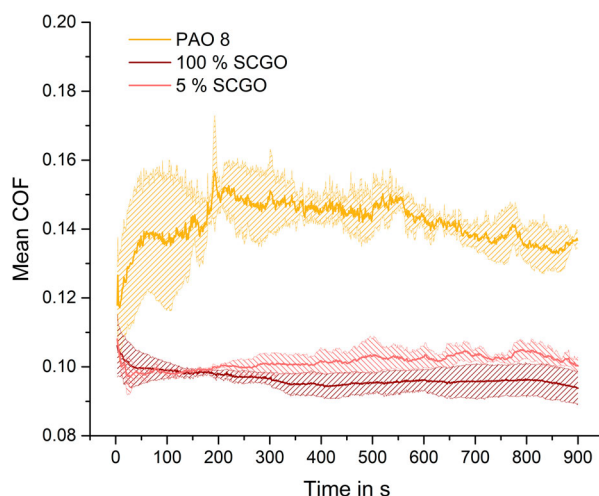

Figure 8. Nanotribometer measurement of COF of different oils on polished S-CRP given with standard deviation between data sets ($n = 3$).

Due to the higher surface roughness of the base body, the surface condition varies within the tested area, which might be the reason for the deviant behavior of 5% SCGO showing a smaller COF than 100% SCGO. The 5% SCGO additive and 100% SCGO samples show good repeatability and better friction stability over the measurement duration.

Nanotribometer experiments on S-CRP samples. Due to the low roughness induced high surface wettability, supposedly only low amounts of lubricant remain within the contact area on polished 100Cr6 surface (S-CRP) compared to the unpolished surfaces of 100Cr6 (S-CRUP) and 1.4301 stainless steel (S-SSUP). As exhibited in Figure 8, this leads to overall higher fluctuation of friction values and higher friction values for PAO 8 ($\mu_{mean} = 0.135$), probably due to the lack of, e.g. ester groups that interact with the metallic surfaces, which are present in 100% SCGO ($\mu_{mean} = 0.094$) and 5% SCGO ($\mu_{mean} = 0.097$).

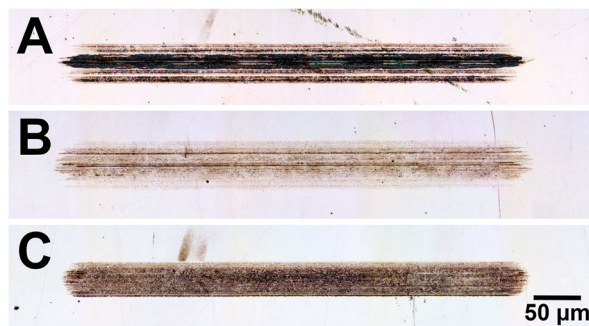Figure 9 shows the difference in wear scar appearance after nanotribometer experiments applying the three

Figure 9. Light microscopic wear scar surface images after nanotribometer experiments of (A) PAO 8, (B) 100% SCGO, and (C) 5% SCGO in PAO 8 on polished S-CRP.

sample lubricants. The wear scar is least pronounced for 100% SCGO, thus being in good agreement with the COF.

Nanotribometer and rheometer experiments on S-CRUP. For the nanotribometer measurements, the lowest COF can be observed for the tribo-experiments on unpolished 100Cr6 discs S-CRUP (Figure 10). Superior to the other materials tested, S-CRUP samples display excellent repeatability with a very low margin of deviation between data points for all three applied lubricants. For this reason, the S-CRUP surface was chosen for further tribological testing on the rheometer. The SCGO exhibits lower COF deriving from long and polar fatty acid chains (μ_{mean} = 0.092 100% SCGO; μ_{mean} = 0.095 5% SCGO; μ_{mean} = 0.129 PAO 8), which are strongly attracted to metallic surfaces. These components are lacking in PAO, a pure hydrocarbon base oil. The ability of SCGO to reduce friction also in the 5% dilution makes it attractive for use as friction modifying boundary lubrication additive. A common friction modifier usually consists of a polar head group and a non-polar tail, creating a cushion between the metal surfaces.

As already identified by the nanotribometer results, the friction-reducing properties of 5% SCGO in PAO 8 compared to pure PAO 8 could be confirmed by the rheometer (Figure 11). The measurements show good repeatability with a low margin of deviation between data points. Generally, the COF on the rheometer versus the nanotribometer is slightly higher but consistent, with COF values of μ_{mean} = 0.114 for 100% SCGO, μ_{mean} = 0.131 for 5% SCGO, and μ_{mean} = 0.163 for PAO 8 for the rheometer. Since the measurement setup on both instruments is quite different, even with aligned parameters, directly comparing the results from the nanotribometer and the rheometer is impossible. This may be due
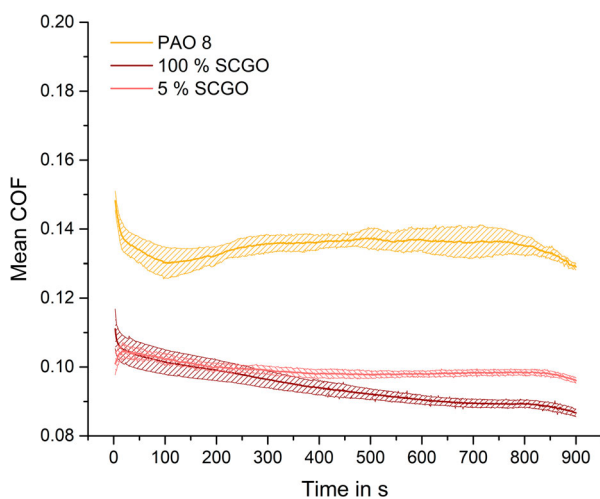

Figure 11. COF of rheometer experiments of different oils on unpolished S-CRUP given with standard deviation between data sets ($n = 2$).

to a better resolution of the nanotribometer with a smaller contact area (2 mm ball) within the 500 μm of testing range than the rheometer (12.7 mm ball).

Rather than only focusing on the COF, the wear volume is also relevant. Characterizing the volume and depth of the wear scar of the different oils with two-dimensional and three-dimensional topographic surface analysis (Table 7), it seemed that PAO 8 generated less wear when surface deposit was forming, leading to a distortion in comparison. This deposit is visible in 3D-topographic images as height increases (red) within the wear scar (Figure 12) and appears as a darkened surface in 2D-microscopy images (Figure 13). Therein; this effect is also slightly visible after experiments using 5% SCGO in PAO 8. Even though 100% SCGO used in rheometer experiments shows the most significant wear scar values, it must be noted that no surface deposit is visible. Instead, a surface polishing effect can be observed in the 2D images for this type of lubricant.

High resolution-MS demonstrated that for all three lubricant sample types, no significant qualitative differences were apparent when comparing pre- (fresh) and post-rheometer test (after two h of duration) samples; therefore, no specific oil degradation products were observed after two h of tribological ageing. In negative

Figure 10. Friction values of nanotribometer experiments of different oils on unpolished S-CRUP given with standard deviation between data sets ($n = 3$).
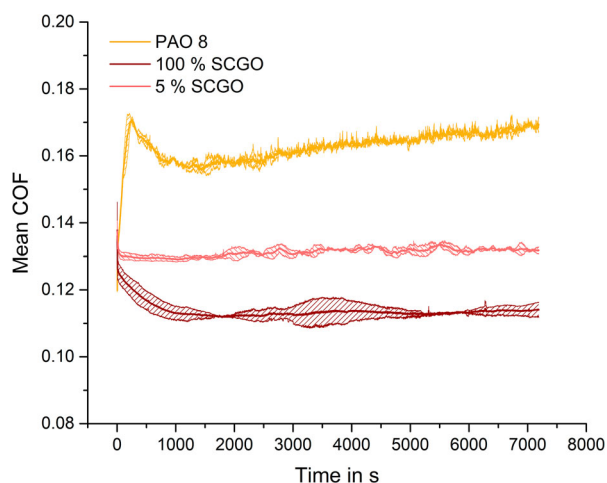
Table 7. Wear track characterisation of unpolished S-CRUP surface after oscillatory rheometer measurements with PAO 8, 100% SCGO and 5% SCGO in PAO 8.

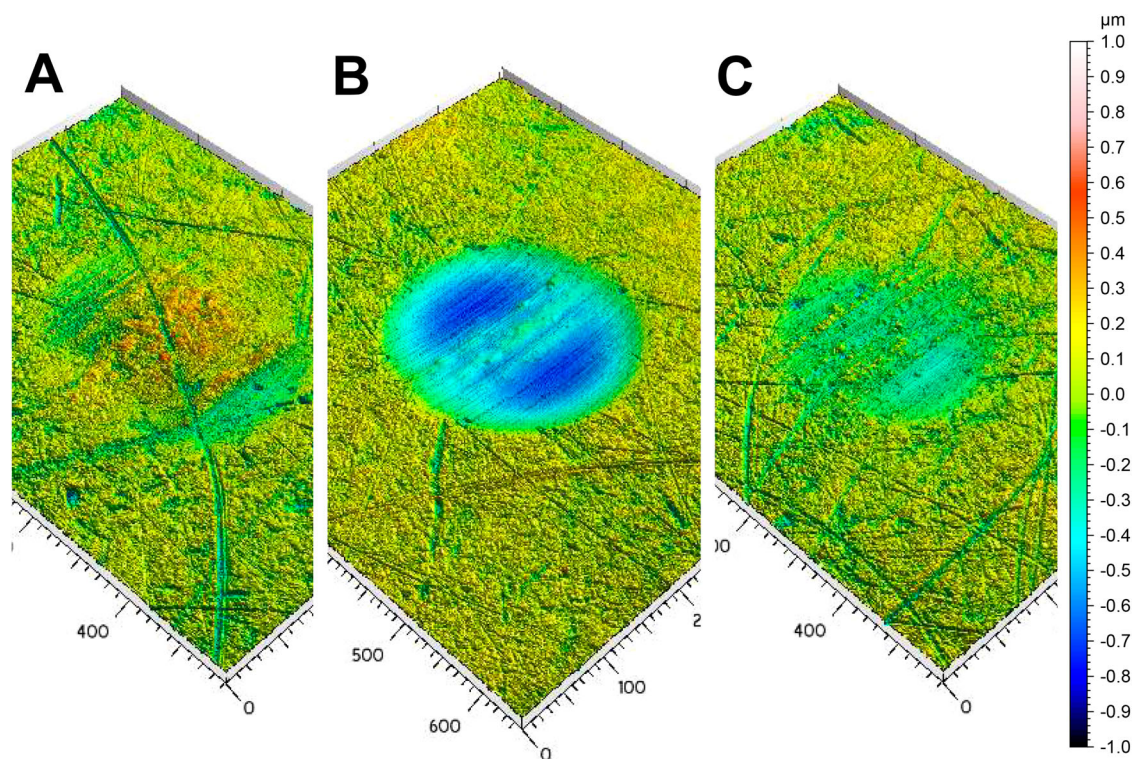|	Linear rheometer experiments (S-CRUP) Mean wear track		
Oil type	Width in μm	Depth in μm	Volume in μm^3
PAO 8	248 ± 9	0.104 ± 0.010	3302 ± 1023
100% SCGO	295 ± 6	0.384 ± 0.021	22638 ± 1910
5% SCGO	228 ± 10	0.140 ± 0.019	4876 ± 889

Figure 12. 3D-topographic surface images of wear tracks after rheometer experiments using (A) PAO 8, (B) 100% SCGO, and (C) 5% SCGO in PAO 8.

ion mode, a reduction in the intensity of about 30% of $C_{10}H_{20}$-groups for PAO 8, 90% of kahweol derivates for 100% SCGO and 50% kahweol palmitate for 5% SCGO in PAO 8 was visible for rheometer tested samples compared to the fresh samples.

Comparing 5% SCGO in PAO 8 and pure PAO 8 rheometer-tested samples, the 5% SCGO could improve the stability of PAO 8 since after tests with pure PAO 8, a loss of intensity of about 30% for the characteristic $C_{10}H_{20}$-groups was observable. In positive mode, glycerides such as mono- (MG), di- (DG), and triglycerides (TG) were visible after tests using 100% SCGO and 5% SCGO

in PAO 8. DG and TG (C16:0, C18:0, C18:1 and C18:3) showed no intensity difference after tests with SCGO as a base lubricant and additive. In contrast, kahweol oleate was reduced by approximately 50% when 100% SCGO and by 70% when 5% SCGO in PAO 8 was applied. Caffeine, also found in the SCGO samples, was reduced by 40% in samples after 100% SCGO was used.

Comparing tested base body materials. Comparisons of the base body materials against 100Cr6 balls under the different oil types investigated are presented in Figure 14, Figure 15 and Figure 16. As can be observed, the unpolished surfaces 1.4301 stainless steel (S-SSUP)
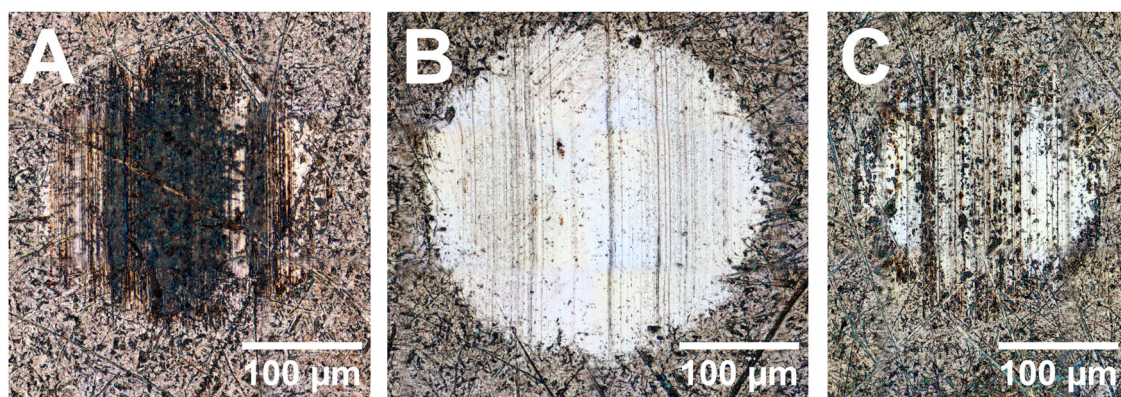

Figure 13. 2D-microscopic surface images of wear tracks after rheometer experiments using (A) PAO 8, (B) 100% SCGO, and (C) 5% SCGO in PAO 8 on unpolished S-CRUP samples.
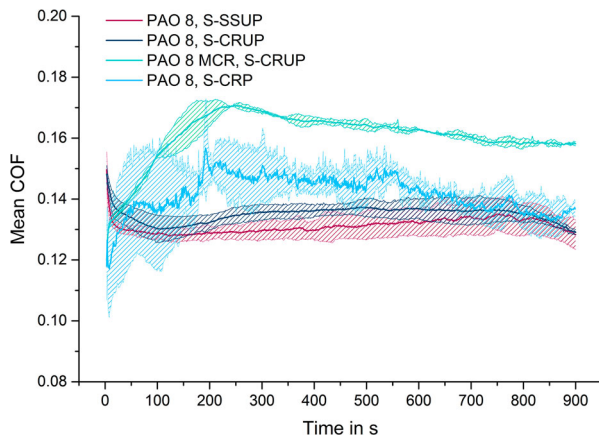
Figure 14. Comparison of friction values for nanotribometer and rheometer experiments applying PAO 8 on different surfaces S-SSUP, S-CRUP, and S-CRP.

and 100Cr6 (S-CRUP) seem to yield more stable friction values compared to the polished 100Cr6 (S-CRP) surface for PAO 8 (probably due to adhesion), for the SCG oils the measurements are very comparable in general. The standard deviation between measurement runs was relatively low, giving high repeatability.

For PAO 8 (Figure 14), the highest COF was reached on the rheometer with the S-CRUP. For the nanotribometer results, S-CRUP and S-SSUP showed quite comparable COF values. The S-CRP surface showed higher fluctuations between measurement repetition, indicating that PAO 8 does not adhere too well to the polished surface.

100% SCGO (Figure 15) shows good repeatability on all three surface types for all measurements. After 15 min of test duration, the COF still decreases, indicating that the materials are in the run-in phase. The lowest COF was reached with the S-CRUP surface, followed by the S-CRP surface for the nanotribometer measurements.
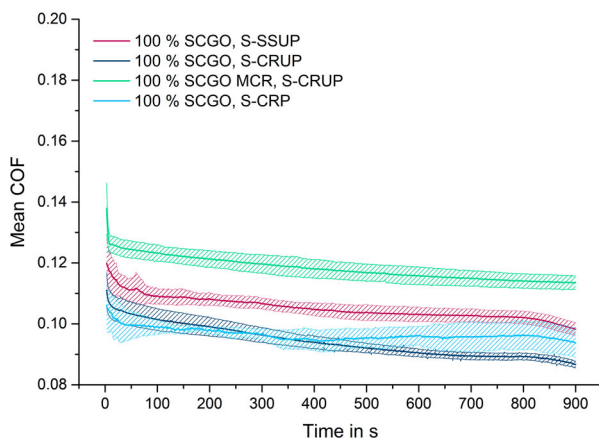

Figure 15. Comparison of friction values for nanotribometer and rheometer experiments applying 100% SCGO on different surfaces S-SSUP, S-CRUP, and S-CRP.
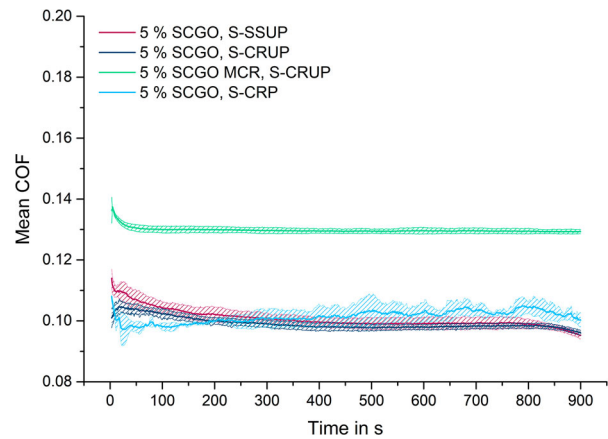

Figure 16. Comparison of friction values for nanotribometer and rheometer experiments applying 5% SCGO compared on different surfaces S-SSUP, S-CRUP, and S-CRP.

For 5% SCGO diluted in PAO 8 (Figure 16), the lowest COF was reached with surfaces S-SSUP and S-CRUP in the nanotribometer measurements. Experiments using S-CRP surfaces showed minor fluctuations, similar to Figure 14, where they are observed to a greater extent. Thus, they seem to derive from PAO 8.

For every oil type applied onto the S-CRUP surface, the measured COFs from experiments on the rheometer are slightly higher than those measured on the nanotribometer. However, a comparison of absolute friction values between instruments is difficult. Due to the differences in the tribo-systems, the contact area in nanotribometer experiments is considerably smaller (2 mm ball; approx. 50 µm of wear track width) and a better resolution based on data acquisition compared to the rheometer (12.7 mm ball; 250-300 µm of wear track width).

Life-cycle assessment case study

A life-cycle assessment (LCA) of oil from SCGs as a future lubricant for the case study of an extruder was undertaken. It includes a scale-up from a lab scale to fit an industrial extruder (operational time 1000 h, with an amount of ∼ 65 l of lubricant). The intention was to assess all tangible environmental impacts associated with various stages of SCGOs' life, ranging from raw material extraction through materials processing, industry size manufacture, distribution, and application. All values are extrapolated from the laboratory scale, including the accompanying uncertainties. For this work, the focus is laid on highlighting especially the critical segments and where process optimization might be necessary.

The LCA is divided into the life-cycle inventory (LCI) conducted with a SimaPro model and the life-cycle impact assessment (LCIA) using the ILCD 2011 Midpoint + Version 1.11 method (specific for Europe). The LCI
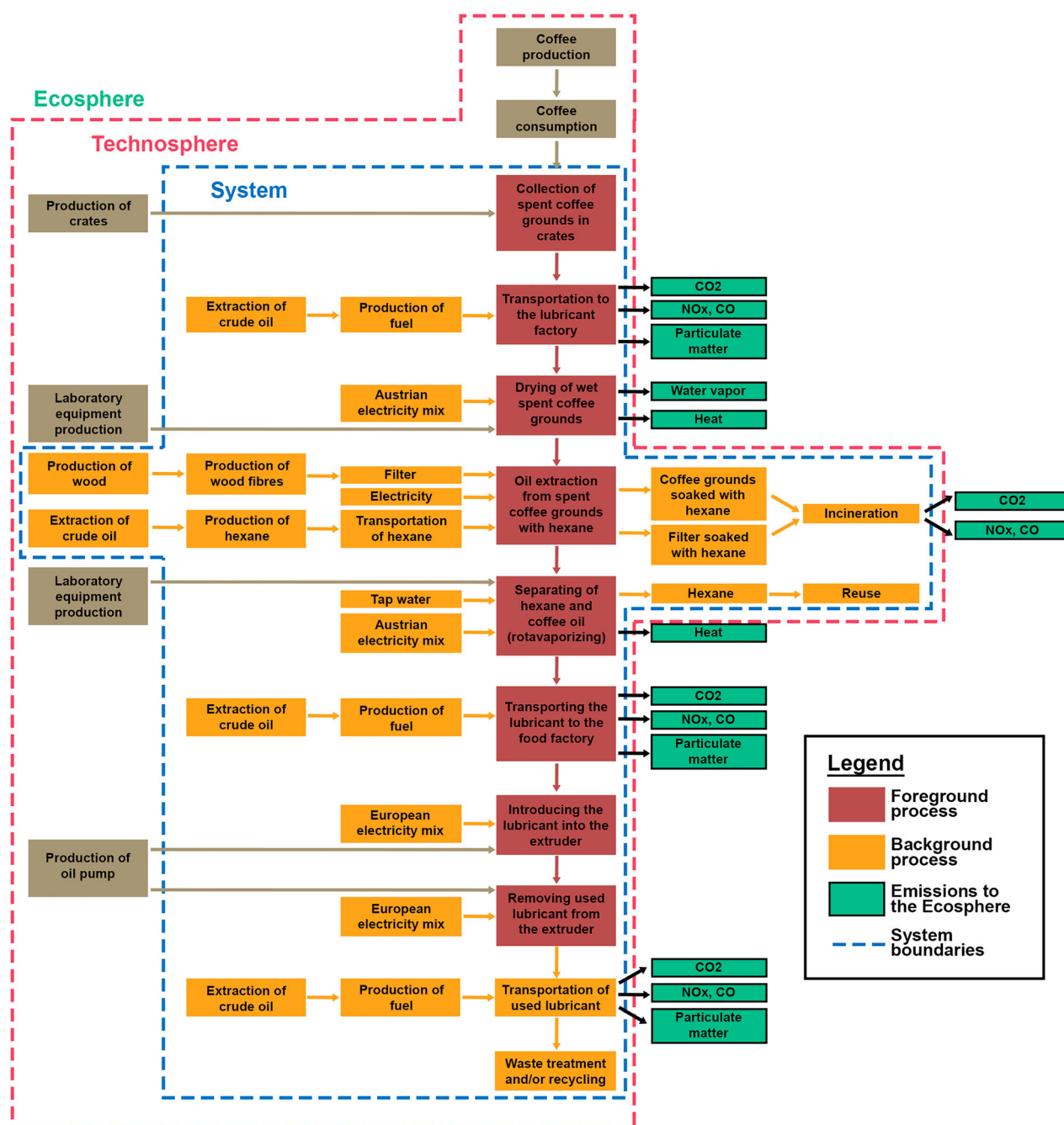
Figure 17. Flow chart of a cradle-to-grave life cycle of SCGO. Adapted with permission from (*23*).

involves the computational model for input and output flows, whereas the LCIA converts these flows into characterized, normalized and weighed impacts (*23*).

Figure 17 displays the whole life cycle of oil collected from SCG, including steps of coffee grounds collection and transportation, manufacturing of oil and further use as 'lubricant' in industrial machinery (certain additives are not taken into account here), as well as the recollection of solvent and disposal of used lubricant (which could be re-refined into base oil in a cradle-to-cradle approach [*24*]).

The four most affected categories (patterned) are shown in Figure 18 and include human toxicity with non-cancerous and cancerous effects, freshwater eutrophication and freshwater ecotoxicity; all derive from n-hexane as the solvent. These impacts originate from n-hexane production, mainly collected during the fractional distillation step of crude mineral oil refining. Furthermore, after extraction, hexane is lost to the environment due to evaporation from paper thimbles and extracted SCGs. This is considered an avoidable output to Technosphere, affecting ozone depletion the
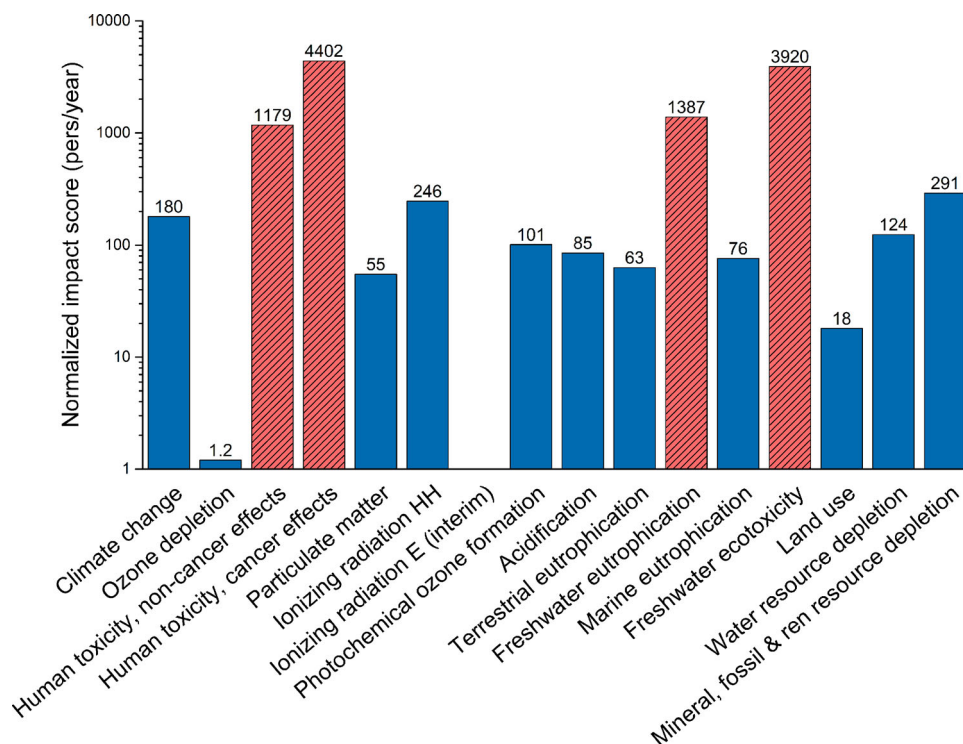
Figure 18. Normalized results of the cradle-to-grave analysis in number of equivalent persons per year (EU27 2010 normalization set) for each midpoint impact category. Adapted with permission from (*23*).

most of all categories (in our model resulting in 261%, with no other impact category exceeding the limit of 30%). A change of n-hexane to a more environmentally friendly solvent could restrict these effects to a minimum extent, which is discussed further in this chapter.

When comparing petroleum-based lubricants with mineral base oil and PAO base oil by a cradle-to-gate LCA approach, PAO performed even worse in all categories, with almost twice the greenhouse gas emissions and generally a more energy-consuming production process. But considering the lubricant lifetime, which is mostly higher for PAO, the impacts are reduced, and mineral oil shows the highest mark in 11 out of 15 categories (*25*).

For the assessment of the oil extraction process, the following three phases and parameters were applied:

(1) *Drying phase*: 105 °C for 24 h, electricity consumption: 4.91 kWh
(2) *Extraction phase*: 140 °C for seven h with hexane as the solvent, electricity consumption: 0.67 kWh
(3) *Rotary evaporation phase*: 50 °C for 1.5 h at 334 mbar, electricity consumption: 2.1 kWh

Values for electricity consumption in phase 3 are based on estimation and might be lower. For phases 1 and 2, the values were measured with a wattmeter.

All data was collected from small scale lab-production, with a collection of approximately 2 g of SCGO from ~ 50 g of wet SCG (~ 15 g of dry SCG).

For the collection of SCGO, the grounds were first dried for 24 h in a drying oven at 105 °C. The LCA demonstrated that the drying process was one of the main impacts concerning energy consumption for the lab-scale setup (including drying, extraction and rotary evaporation).

According to the results of TGA/DSC (Figure 19), the sample (~ 40 mg) was thoroughly dried after 16 min
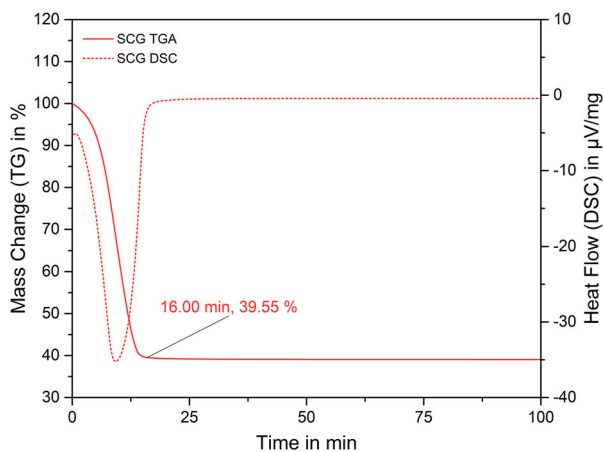

Figure 19. Drying rate of SCGs with TGA/DSC.

with 60.45% water evaporation. Stirring the sample during drying could even improve that process. Since SCGs are dried in more significant portions (∼ 40 g) in the drying oven, the result of the TGA cannot be transferred directly, but the drying time might still be reduced by one order of magnitude. Furthermore, at an industrial scale, water vapor from the exhaust air stream could be re-collected in an exhaust head and reused.

The drying process was discussed as an energy-intensive process by Mabona et al. (19), which is why they assessed the dependence of moisture content on SCGO yields. They extracted SCGs with up to 20 wt% of residual moisture in non-polar solvents (hexane, toluene) and 40 wt% in polar solvents (ethanol, acetone). High moisture content was limiting for non-polar solvents, which might fail to access the SCGs properly. In contrast, polar solvents could extract more significant amounts of SCGO with higher initial water content. The best results were given by ethanol at 40 wt% with over 20% of oil yield, higher moisture contents were considered limiting. Choosing ethanol over hexane as an extraction solvent would result in a more environmentally friendly extraction process.

For the life-cycle assessment, the drying process has the most significant impact on electric power consumption. However, using n-hexane as the solvent for the extraction process introduces increased human- and eco-toxicity and freshwater eutrophication values. In addition, n-hexane evaporating from the residual waste coffee grounds after the extraction step might impact ozone depletion when not re-collected and/or disposed of properly. This conclusion is cautiously based on a direct up-scaling from the lab- to the industrial scale. Thus, a comprehensive argumentation is yet to be feasible at this point. For future LCA approaches, models could be considered, including adapted industrial process structures and more reliable values (electricity consumption, SCG amount, oil yields, etc.) for an industrial production scale.

Conclusion

This work took a further step toward understanding the tribological applicability of waste-based SCGOs. For the first time, a broad approach to evaluate the tribological behavior of SCGO was deployed, and a wide range of tribological experiments applying SCGO was performed.

Based on experimental results, SCGO can reduce the friction coefficient as a pure oil and applied as a 5% additive in PAO 8, the latter being a common synthetic base oil that served as a reference in this study. The lowest

COF and most stable friction behavior could be reached when 100% SCGO was applied on unpolished 100Cr6 (S-CRUP) samples due to ester groups within the oil that positively affect the COF. The best results for 5% SCGO in PAO 8 and pure PAO 8 were also achieved with the same surface. Therein, it could be proven that SCGO has tremendous potential when used as a base lubricant and as a friction modifier additive in a standard industrial base oil, especially when compared to PAO 8 as the reference lubricant. This outcome could interest various industrial applications, from the automotive industry to machines used, e.g. for food production.

To increase comprehension of SCGO functionalities and their influence on friction and wear, future investigations could include (a) further decreasing the amount of SCGO used as an additive without adversely affecting friction and wear modification properties (to maximize resource efficiency); (b) altering SCGOs under defined conditions for simulations of industrial applications, e.g. engine, bearing or pump devices; (c) exploring the applicable operational ranges of SCGO in tribo-tests; (d) using eco-friendly, sustainable base oils and references; (e) improving the extraction pathway to be more energy efficient; (f) estimation of environmental impact by performing biodegradability, bioaccumulation, and toxicity tests; and (g) assessment of valid values for industrial economy throughout the life cycle of SCGO.

Disclosure statement

No potential conflict of interest was reported by the author(s).

ORCID

Rosa Maria Eder http://orcid.org/0009-0002-3624-8422
Lukas Widder http://orcid.org/0000-0001-8297-8966
Markus Varga http://orcid.org/0000-0001-8272-4122
Martina Marchetti-Deschmann http://orcid.org/0000-0002-8060-7851
Marcella Frauscher http://orcid.org/0000-0001-7939-9656

References

[1] L. R. Rudnick, In *Synthetics, Mineral Oils, and Bio-Based Lubricants*, L. R. Rudnick, Ed.; CRC Press: Boca Raton, FL, 2020. doi:10.1201/9781315158150.

[2] United States Department of Agriculture (USDA), "BioPreferred® Program", [Online]. https://www.biopreferred.gov/BioPreferred/ (accessed Jan 12, 2022).

[3] European Commission. Regulation (EU) 2018/1999 of the European Parliament and of the Council of 11 December 2018 on the Governance of the Energy Union and Climate Action, Amending Regulations (EC) No 663/2009 and (EC) No 715/2009 of the European Parliament and of the Council, Directives 94/22/EC, 98/70/EC, 2009/31/EC, 2009/73/EC, 2010/31/EU, 2012/27/EU and 2013/30/EU of the European Parliament and of the Council, Council Directives 2009/119/EC and (EU) 2015/652 and repealing Regulation (EU) No 525/2013 of the European Parliament and of the Council (Text with EEA relevance.). *Off. J. Eur. Union* **2018,** *328*, 1–77.

[4] European Union, "A European Green Deal, Striving to be the First Climate-Neutral Continent", [Online]. https://ec.europa.eu/info/strategy/priorities-2019-2024/european-green-deal_en. (accessed Jan 12, 2022).

[5] Ibanez, J.; Martín, S.M.; Baldino, S.; Prandi, C.; Mannu, A. European Union Legislation Overview about Used Vegetable Oils Recycling: The Spanish and Italian Case Studies. *Processes* **2020,** *8*, 798. doi:10.3390/pr8070798.

[6] European Commission. Directive (EU) 2018/851 of the European Parliament and of the Council of 30 May 2018 amending Directive 2008/98/EC on waste (Text with EEA relevance). *Off. J. Eur. Union* **2018**, 1–32.

[7] European Commission, "Circular Economy: New rules will make EU the global front-runner in waste management and recycling". [Online]. https://ec.europa.eu/commission/presscorner/detail/en/IP_18_3846. (accessed Oct 7, 2020), 2018.

[8] European Commission. Regulation (EC) No 66/2010 of the European Parliament and of the Council of 25 November 2009 on the EU Ecolabel (Text with EEA Relevance). *Off. J. Eur. Union* **2010,** *27*, 1–19.

[9] Tchibo and A. Liedtke, "Kaffee in Zahlen No. 9", Brand Eins. [Online]. https://de.statista.com/statistik/studie/id/75371/dokument/kaffee-in-zahlen-2020/. (accessed Jan 12, 2022), 2020.

[10] I. Efthymiopoulos, "Recovery of Lipids from Spent Coffee Grounds for use as a Biofuel", London, 2018.

[11] Abdullah, M.; Koc, A.B. Oil Removal From Waste Coffee Grounds Using Two-Phase Solvent Extractionenhanced With Ultrasonication. *Renew. Energy* **2013,** *50*, 965–970. doi:10.1016/j.renene.2012.08.073.

[12] Calixto, F.; Fernandes, J.; Couto, R.; Hernández, E.J.; Najdanovic-Visak, V.; Simões, P.C. Synthesis of Fatty Acid Methyl Esters via Direct Transesterification with Methanol/Carbon Dioxide Mixtures from Spent Coffee Grounds Feedstock. *Green Chem.* **2011,** *13*, 1196. doi:10.1039/c1gc15101k.

[13] Vardon, D.R.; Moser, B.R.; Zheng, W.; Witkin, K.; Evangelista, R.L.; Strathmann, T.J.; Rajagopalan, K.; Sharma, B.K. Complete Utilization of Spent Coffee Grounds To Produce Biodiesel, Bio-Oil, and Biochar. *ACS Sustain. Chem. Eng.* **2013,** *1*, 1286–1294. doi:10.1021/sc400145w.

[14] Uddin, M.N.; Techato, K.; Rasul, M.G.; Hassan, N.M.S.; Mofijur, M. Waste Coffee oil: A Promising Source for Biodiesel Production. *Energy Procedia* **2019,** *160*, 677–682. doi:10.1016/j.egypro.2019.02.221.

[15] Andrade, K.S.; Gonçalvez, R.T.; Maraschin, M.; do-Valle, R.M.R.; Martínez, J.; Ferreira, S.R.S. Supercritical Fluid Extraction from Spent Coffee Grounds and Coffee Husks: Antioxidant Activity and Effect of Operational Variables on Extract Composition. *Talanta* **2012,** *88*, 544–552. doi:10.1016/j.talanta.2011.11.031.

[16] Ciesielczuk, T.; Rosik-Dulewska, C.; Poluszyńska, J.; Miłek, D.; Szewczyk, A.; Sławińska, I. Acute Toxicity of Experimental Fertilizers Made of Spent Coffee Grounds. *Waste Biomass Valoriz.* **2017,** *9*, 2157–2164. doi:10.1007/s12649-017-9980-3.

[17] Grace, J.; Vysochanska, S.; Lodge, J.; Iglesias, P. Ionic Liquids as Additives of Coffee Bean Oil in Steel-Steel Contacts. *Lubricants* **2015,** *3*, 637–649. doi:10.3390/lubricants3040637.

[18] Al-Hamamre, Z.; Foerster, S.; Hartmann, F.; Kröger, M.; Kaltschmitt, M. Oil Extracted from Spent Coffee Grounds as a Renewable Source for Fatty Acid Methyl Ester Manufacturing. *Fuel* **2012,** *96*, 70–76. doi:10.1016/j.fuel.2012.01.023.

[19] Mabona, N.; Aboyade, W.; Mollagee, M.; Mguni, L.L. Effect of Moisture Content on oil Extraction from Spent Coffee Grounds. *Energy Sourc. Part A: Recov. Utiliz. Environ. Effects* **2018,** *40*, 501–509. doi:10.1080/15567036.2014.915361.

[20] Ahangari, B.; Sargolzaei, J. Extraction of Lipids from Spent Coffee Grounds Using Organic Solvents and Supercritical Carbon Dioxide. *J. Food Process. Preserv.* **2013,** *37*, 1014–1021. doi:10.1111/j.1745-4549.2012.00757.x.

[21] Hibbert, S.; Welham, K.; Zein, S.H. An Innovative Method of Extraction of Coffee oil Using an Advanced Microwave System: In Comparison with Conventional Soxhlet Extraction Method. *SN Appl. Sci.* **2019**, *1*. doi:10.1007/s42452-019-1457-5.

[22] Unugul, T.; Kutluk, T.; Kutluk, B.G.; Kapucu, N. Environmentally Friendly Processes from Coffee Wastes to Trimethylolpropane Esters to be Considered Biolubricants. *J. Air Waste Manag. Assoc.* **2020,** *70*, 1198–1215. doi:10.1080/10962247.2020.1788664.

[23] A. Müller, A. Deli, C. Delafargue, C. Martzakli, M. Grangé and S. Hvidkjær, "Lubricant Oil from Spent Coffee Grounds", Unpublished document of Technical University of Denmark, Lyngby, 2021.

[24] J. Sander, "Lubricants Can't Be Green … Can They?", Lubrication Engineers, Inc.. [Online]. Available: https://www.lelubricants.com/wp-content/uploads/pdf/news/White%20Papers/Green%20Lubricants%20white%20paper.pdf. (accessed Jul 18, 2022), 2017.

[25] Raimondi, A.; Girotti, G.; Blengini, G.A.; Fino, D. LCA of Petroleum-Based Lubricants: State of art and Inclusion of Additives. *Intern. J. Life Cycle Assess.* **2012,** *17*, 987–996. doi:10.1007/s11367-012-0437-4.